

Numerical approach for high precision 3D relativistic star models

Silvano Bonazzola,^{*} Ericourgoulhon,[†] and Jean-Alain Marck[‡]

Département d'Astrophysique Relativiste et de Cosmologie, UPR 176 du CNRS, Observatoire de Paris, F-92195 Meudon Cedex, France

(Received 10 February 1998; published 20 October 1998)

A multidomain spectral method for computing very high precision three-dimensional stellar models is presented. The boundary of each domain is chosen in order to coincide with a physical discontinuity (e.g., the star's surface). In addition, a regularization procedure is introduced to deal with the infinite derivatives on the boundary that may appear in the density field when stiff equations of state are used. Consequently all the physical fields are smooth functions on each domain and the spectral method is absolutely free of any Gibbs phenomenon, which yields to a very high precision. The power of this method is demonstrated by direct comparison with analytical solutions such as MacLaurin spheroids and Roche ellipsoids. The relative numerical error is revealed to be of the order of 10^{-10} . This approach has been developed for the study of relativistic inspiralling binaries. It may be applied to a wider class of astrophysical problems such as the study of relativistic rotating stars too. [S0556-2821(98)06318-8]

PACS number(s): 04.25.Dm, 02.60.Cb, 02.70.Hm

I. INTRODUCTION

One of the most promising sources of gravitational waves is the coalescence of inspiralling compact binaries. The recent development of interferometric gravitational waves detectors [e.g., GEO600, Laser Interferometric Gravitational Wave Observatory (LIGO), TAMA, and VIRGO] gives an important motivation for studying this problem. Such a study requires a relativistic formalism to derive the equations of motion and then an accurate and tricky method to solve the resulting system of partial differential equations. We have recently [1] proposed a relativistic formalism able to tackle the problem of corotating *as well as* counter-rotating binaries system, the latter being more relevant from the astrophysical point of view. We present now a very accurate approach based on the multidomain spectral method that circumvents the Gibbs phenomenon to numerically solve this problem and which can be applied to a wide class of other astrophysical situations.

Various astrophysical applications of spectral methods have been developed in our group (for a review, see Ref. [2]), including three-dimensional (3D) gravitational collapse of stellar core [3], neutron star collapse into a black hole [4–7], tidal disruption of a star near a massive black hole [8], rapidly rotating neutron stars [9–12], magnetized neutron stars [13,14] and their resulting gravitational radiation [15], spontaneous symmetry breaking of rapidly rotating neutron stars [16,17], and protoneutron star evolution [18–20].

In computational fluid dynamics, spectral methods are known for their very high accuracy [21,22]; indeed for a C^∞ function, the numerical error decreases as $\exp(-N)$ (*evanescent error*), where N is the number of coefficients involved in the spectral expansion, or equivalently the number of grid points in the physical domain. This is much faster than the

error decay of finite-difference methods, which behaves as $1/N^q$, with q generally not larger than 3. For this reason, spectral methods are particularly interesting for treating 3D problems—such as binary configurations—a situation in which the number of grid points is still severely limited by the capability of present and next generation computers.

Spectral methods lose much of their accuracy when non-smooth functions are treated because of the so-called Gibbs phenomenon. This phenomenon is well known from the most familiar spectral method, namely, the theory of Fourier series: the Fourier coefficients (c_n) of a function f which is of class C^p but not C^{p+1} decrease as $1/n^p$ only. In particular, if the function has some discontinuity, its approximation by a Fourier series does not converge towards f at the discontinuity point: there remains a gap which is of the order 10%.

The multidomain spectral method described in this paper circumvents the Gibbs phenomenon. The basic idea is to divide the space into domains chosen so that the physical discontinuities are located onto the boundaries between the domains (Sec. II). The simplest example is the case of a perfect fluid star, where two domains may be distinguished: the interior and the exterior of the star. The boundary is then simply the surface of the star. The second ingredient of the technique is a mapping between the domains defined in this way and some simple mathematical domains, which are cross products of intervals: $[a_1, a_2] \times [b_1, b_2] \times [c_1, c_2]$. The spectral expansion is then performed with respect to functions of the coordinates spanning these intervals (Sec. III). The method of resolution of a basic equation, namely, the Poisson equation, is exposed in Sec. III C. For stiff equations of state, the above procedure is not sufficient to ensure the smoothness of all the functions. Indeed, for a polytrope with an adiabatic index greater than 2, the density field has an infinite derivative on the surface of the star. We present in Sec. IV a method for regularizing the density and recover the spectral precision. The power of the multidomain spectral method is illustrated in Sec. V, where comparisons are performed between numerical solutions obtained by an implementation of the method and analytical solutions (ellipsoidal

^{*}Email address: bona@mesio.observatoire.fr

[†]Email address: Eric.Gourgoulhon@obspm.fr

[‡]Email address: Jean-Alain.Marck@obspm.fr

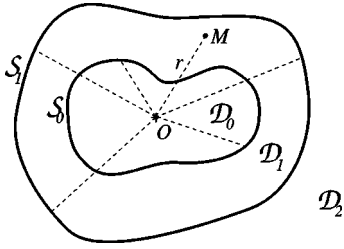


FIG. 1. Splitting of the physical three-dimensional space into domains $\mathcal{D}_0, \mathcal{D}_1, \dots, \mathcal{D}_{\mathcal{N}-1}$ (on the figure $\mathcal{N}=3$), which are starlike with respect to some origin O . The last domain (here \mathcal{D}_2) extends up to infinity.

configurations of incompressible fluids). Finally Sec. VI concludes the article by discussing the great advantages of the multidomain spectral method for dealing with relativistic binary neutron stars.

II. THE PHYSICAL DOMAINS AND THEIR MAPPING

A. Splitting of the physical space into starlike domains

In order to treat problems involving Poisson equations with non-compact sources—as they appear in relativistic gravitation—we take for the physical domain where the computation must be performed the whole three-dimensional space \mathbb{R}^3 . In doing so, we know the physical boundary conditions we have to impose in order to solve the Poisson equations. These boundary conditions can be easily set at infinity. We divide \mathbb{R}^3 into \mathcal{N} domains $(\mathcal{D}_l)_{0 \leq l \leq \mathcal{N}-1}$ ($\mathcal{N} \geq 2$). In the present work, these domains are taken to be *starlike* (in the mathematical sense) with respect to a some origin O , which means that for every point M in the domain \mathcal{D}_l , the segment OM is entirely included in $\cup_{i \leq l} \mathcal{D}_i$ (see Fig. 1). The multidomain spectral method we are going to describe can be extended to more general domains, at the price of a greater technical (but nonconceptual) difficulty. However, for stellar configurations, the starlike hypothesis is sufficient for most applications. Let us denote by S_l the boundary surface between the domains \mathcal{D}_l and \mathcal{D}_{l+1} . \mathcal{D}_0 is simply connected and its boundary is S_0 ; we call it the nucleus. For $1 \leq l \leq \mathcal{N}-2$, \mathcal{D}_l 's inner boundary is S_{l-1} and outer boundary S_l . The last domain $\mathcal{D}_{\mathcal{N}-1}$ has $S_{\mathcal{N}-2}$ as inner boundary and extends to infinity (see Fig. 1).

Let us choose some Cartesian frame of \mathbb{R}^3 centered at O and let us call (r, θ, φ) the associated spherical coordinates $r \in [0, +\infty[$, $\theta \in [0, \pi]$ and $\varphi \in [0, 2\pi[$. The mapping of each domain onto the cross product of intervals $[a_1, a_2] \times [b_1, b_2] \times [c_1, c_2]$ will be defined with respect to the spherical coordinates (r, θ, φ) . Since each domain \mathcal{D}_l is starlike with respect to O , the equation of the boundaries S_l can be written in the form

$$r = S_l(\theta, \varphi), \quad (1)$$

where S_l is a smooth function on $[0, \pi] \times [0, 2\pi[$.

B. Mapping of the nucleus

The basic idea is to introduce the mapping

$$[0, 1] \times [0, \pi] \times [0, 2\pi[\rightarrow \mathcal{D}_0, \quad (\xi, \theta', \varphi') \mapsto (r, \theta, \varphi) \quad (2)$$

so that the origin O corresponds to $\xi=0$ and the boundary S_0 to $\xi=\text{const}=1$. Using the fact that \mathcal{D}_0 is starlike, a simple form of the mapping (2) can be chosen as

$$r = R_0(\xi, \theta', \varphi'), \quad (3)$$

$$\theta = \theta', \quad (4)$$

$$\varphi = \varphi', \quad (5)$$

where R_0 is a smooth function subject to regularity properties which are discussed below. Thanks to Eqs. (4), (5), we will make no distinction between θ and θ' , as well as between φ and φ' , i.e., we will abandon the primes on the angles. The fact that \mathcal{D}_0 's boundary coincides with $\xi=1$ translates as

$$R_0(1, \theta, \varphi) = S_0(\theta, \varphi). \quad (6)$$

In addition to Eq. (6), the function R_0 must satisfy some regularity properties induced by the singular behavior of spherical coordinates at $r=0$, $\theta=0$, and $\theta=\pi$. We define a function $f: \mathbb{R}^3 \rightarrow \mathbb{R}$ to be regular if it can be expressed as a polynomial of the Cartesian coordinates

$$x = r \sin \theta \cos \varphi, \quad (7)$$

$$y = r \sin \theta \sin \varphi, \quad (8)$$

$$z = r \cos \theta. \quad (9)$$

We will assume that all the physical fields are regular functions on each domain \mathcal{D}_l (the domains \mathcal{D}_l are in fact chosen in this manner) with respect to the previous definition. It is easy to see that any regular function is expandable as

$$f(r, \theta, \varphi) = \sum_{m=-M}^M \sum_{\ell=|m|}^L r^\ell T(r^2) \sin^{|m|} \theta P_{\ell-|m|}(\cos \theta) e^{im\varphi}, \quad (10)$$

where L and M are positive integers, $L \geq M$, $P_{\ell-|m|}$ is some polynomial of degree $\ell-|m|$ and $T(r^2)$ is some even polynomial.

A simple form of the mapping (3)–(5) has already been introduced in the literature [23–25], namely, $R_0(\xi, \theta, \varphi) = S_0(\theta, \varphi)\xi$, where $S_0(\theta, \varphi)$ is the equation of the star's surface [Eq. (1)]. However, for such a mapping the regularity condition (10) would be quite complicated when expressed in terms of (ξ, θ, φ) . We choose instead the mapping defined by

$$R_0(\xi, \theta, \varphi) = \alpha_0 [\xi + A_0(\xi)F_0(\theta, \varphi) + B_0(\xi)G_0(\theta, \varphi)], \quad (11)$$

where A_0 and B_0 are the following even and odd polynomials:

$$A_0(\xi) = 3\xi^4 - 2\xi^6, \quad (12)$$

$$B_0(\xi) = (5\xi^3 - 3\xi^5)/2, \quad (13)$$

and the constant α_0 as well as the two functions $F_0(\theta, \varphi)$ and $G_0(\theta, \varphi)$ are such that (i) the Fourier expansion of $F_0(\theta, \varphi)$ [$G_0(\theta, \varphi)$] with respect to φ contains only even [odd] harmonics and (ii) the equation of the surface S_0 can be written

$$\alpha_0[1 + F_0(\theta, \varphi) + G_0(\theta, \varphi)] = S_0(\theta, \varphi). \quad (14)$$

The polynomials A_0 and B_0 defined by Eqs. (12), (13) are such that

$$A_0(0) = B_0(0) = 0, \quad (15)$$

$$A'_0(0) = B'_0(0) = 0, \quad (16)$$

$$A_0(1) = B_0(1) = 1, \quad (17)$$

$$A'_0(1) = B'_0(1) = 0. \quad (18)$$

The properties (14) and (17) ensure that Eq. (6) is satisfied, i.e., that the mapping (11) is from $[0, 1] \times [0, \pi] \times [0, 2\pi[$ to \mathcal{D}_0 . The polynomials A_0 and B_0 are chosen in order to satisfy at the minimum level the regularity conditions mentioned above. In particular, near the origin r behaves as $r \sim \alpha_0 \xi$ and is independent of (θ, φ) , which would not have been the case of the mapping $r = S_0(\theta, \varphi)$ ξ introduced in Refs. [23–25].

The Jacobian of the transformation $(r, \theta, \varphi) \mapsto (\xi, \theta, \varphi)$ is

$$J := \frac{\partial(r, \theta, \varphi)}{\partial(\xi, \theta, \varphi)} = \frac{\partial R_0}{\partial \xi} \\ = \alpha_0[1 + A'_0(\xi)F_0(\theta, \varphi) + B'_0(\xi)G_0(\theta, \varphi)]. \quad (19)$$

Since $A'_0(\xi) \geq 0$ and $B'_0(\xi) \geq 0$ for any $\xi \in [0, 1]$, the mapping could become singular if $F_0(\theta, \varphi)$ or $G_0(\theta, \varphi)$ is negative and has an important amplitude. We cannot control the sign of the function $F_0(\theta, \varphi)$ because it contains only odd harmonics of φ . However, by a suitable choice of α_0 , one can impose

$$G_0(\theta, \varphi) \geq 0, \quad (20)$$

as we shall see below. We have found that this condition was sufficient to ensure that $J \neq 0$, i.e., that the mapping is regular, for all the astrophysically relevant situations we have encountered.

The equation for the surface of the domain \mathcal{D}_0 having been given, in the form of Eq. (1), $r = S_0(\theta, \varphi)$, so the procedure which leads to α_0 , $F_0(\theta, \varphi)$, and $G_0(\theta, \varphi)$, i.e., to the full determination of the function $R_0(\xi, \theta, \varphi)$, is the following one. First let us choose a point (θ_*, φ_*) on the surface S_0 . Equation (14) implies the following relation:

$$\alpha_0[1 + F_0(\theta_*, \varphi_*) + G_0(\theta_*, \varphi_*)] = S_0(\theta_*, \varphi_*). \quad (21)$$

Let us introduce the following auxiliaries quantities:

$$\mu := \alpha_0[F_0(\theta_*, \varphi_*) + G_0(\theta_*, \varphi_*)], \quad (22)$$

$$\tilde{F}_0(\theta, \varphi) := \alpha_0 F_0(\theta, \varphi), \quad (23)$$

$$\tilde{G}_0(\theta, \varphi) := \alpha_0 G_0(\theta, \varphi) - \mu. \quad (24)$$

Equation (21) then translates as

$$\alpha_0 + \mu = S_0(\theta_*, \varphi_*), \quad (25)$$

whereas Eq. (14) becomes

$$\tilde{F}_0(\theta, \varphi) + \tilde{G}_0(\theta, \varphi) = S_0(\theta, \varphi) - S_0(\theta_*, \varphi_*). \quad (26)$$

Having expanded $f(\theta, \varphi) := S_0(\theta, \varphi) - S_0(\theta_*, \varphi_*)$ into Fourier series with respect to φ , one deduces the functions $\tilde{F}_0(\theta, \varphi)$ [$\tilde{G}_0(\theta, \varphi)$] by taking only the odd [even] harmonics of this Fourier expansion. μ is then computed as

$$\mu = -\min\{\tilde{G}_0(\theta, \varphi), (\theta, \varphi) \in [0, \pi] \times [0, 2\pi[\}. \quad (27)$$

In doing so, condition (20) will automatically be satisfied. The value of the coefficient α_0 is deduced from the above value of μ via Eq. (25). Finally the functions $F_0(\theta, \varphi)$ and $G_0(\theta, \varphi)$ are computed from Eqs. (23) and (24).

C. Mapping of the intermediate domains

For $1 \leq l \leq \mathcal{N} - 2$, we introduce the mapping

$$[-1, 1] \times [0, \pi] \times [0, 2\pi[\rightarrow \mathcal{D}_l, \\ (\xi, \theta', \varphi') \mapsto (r, \theta, \varphi) \quad (28)$$

under the form

$$r = R_l(\xi, \theta', \varphi'), \quad (29)$$

$$\theta = \theta', \quad (30)$$

$$\varphi = \varphi', \quad (31)$$

where R_l is a smooth function which satisfies

$$R_l(-1, \theta, \varphi) = S_{l-1}(\theta, \varphi), \quad (32)$$

$$R_l(+1, \theta, \varphi) = S_l(\theta, \varphi), \quad (33)$$

which means that the inner (outer) boundary of \mathcal{D}_l is defined by $\xi = -1$ ($\xi = +1$).

We choose $R_l(\xi, \theta, \varphi)$ as

$$R_l(\xi, \theta, \varphi) = \alpha_l[\xi + A_l(\xi)F_l(\theta, \varphi) + B_l(\xi)G_l(\theta, \varphi)] + \beta_l, \quad (34)$$

where A_l and B_l are the following polynomials:

$$A_l(\xi) = (\xi^3 - 3\xi + 2)/4, \quad (35)$$

$$B_l(\xi) = (-\xi^3 + 3\xi + 2)/4, \quad (36)$$

and the constants α_l and β_l and the two functions $F_l(\theta, \varphi)$ and $G_l(\theta, \varphi)$ are defined from the equations of the surfaces S_{l-1} and S_l by

$$\alpha_l[-1 + F_l(\theta, \varphi)] + \beta_l = S_{l-1}(\theta, \varphi), \quad (37)$$

$$\alpha_l[+1 + G_l(\theta, \varphi)] + \beta_l = S_l(\theta, \varphi), \quad (38)$$

$$F_l(\theta, \varphi) \leq 0, \quad (39)$$

$$G_l(\theta, \varphi) \geq 0. \quad (40)$$

Note that the polynomials A_l and B_l defined by Eqs. (35), (36) are such that

$$A_l(-1) = 1 \quad \text{and} \quad B_l(-1) = 0, \quad (41)$$

$$A_l(+1) = 0 \quad \text{and} \quad B_l(+1) = 1, \quad (42)$$

$$A'_l(-1) = B'_l(-1) = A'_l(+1) = B'_l(+1) = 0. \quad (43)$$

The properties (37) and (41) [(38) and (42)] ensure that Eq. (32) [Eq. (33)] is satisfied, i.e., that the mapping (34) is from $[-1, 1] \times [0, \pi] \times [0, 2\pi[$ to \mathcal{D}_l . The conditions (39) and (40) ensure that this mapping is not singular, by the same argument as that presented for R_0 in Sec. II B, the sign of $F_l(\theta, \varphi)$ being opposite to that of $G_l(\theta, \varphi)$ because A_l is a decreasing function of ξ , whereas B_l is an increasing function of ξ .

The equation for the inner and outer boundaries of the domain \mathcal{D}_l being given, in the form of Eq. (1): $r = S_{l-1}(\theta, \varphi)$ (inner boundary) and $r = S_l(\theta, \varphi)$ (outer boundary), the procedure which leads to α_l , β_l , $F_l(\theta, \varphi)$, and $G_l(\theta, \varphi)$, i.e., to the full determination of the function $R_l(\xi, \theta, \varphi)$, is the following one. First let us choose a point (θ_*, φ_*) on the surface S_{l-1} along with the corresponding point (θ_*, φ_*) on the surface S_l . Equations (37) and (38) imply the following relations:

$$\alpha_l[-1 + F_l(\theta_*, \varphi_*)] + \beta_l = S_{l-1}(\theta_*, \varphi_*), \quad (44)$$

$$\alpha_l[+1 + G_l(\theta_*, \varphi_*)] + \beta_l = S_l(\theta_*, \varphi_*). \quad (45)$$

Let us introduce the following auxiliaries quantities:

$$\lambda := \alpha_l F_l(\theta_*, \varphi_*), \quad (46)$$

$$\mu := \alpha_l G_l(\theta_*, \varphi_*), \quad (47)$$

$$\tilde{F}_l(\theta, \varphi) := \alpha_l F_l(\theta, \varphi) - \lambda, \quad (48)$$

$$\tilde{G}_l(\theta, \varphi) := \alpha_l G_l(\theta, \varphi) - \mu. \quad (49)$$

Equations (44) and (45) then translate as

$$-\alpha_l + \lambda + \beta_l = S_{l-1}(\theta_*, \varphi_*), \quad (50)$$

$$\alpha_l + \mu + \beta_l = S_l(\theta_*, \varphi_*), \quad (51)$$

whereas Eqs. (37) and (38) become

$$\tilde{F}_l(\theta, \varphi) = S_{l-1}(\theta, \varphi) - S_{l-1}(\theta_*, \varphi_*), \quad (52)$$

$$\tilde{G}_l(\theta, \varphi) = S_l(\theta, \varphi) - S_l(\theta_*, \varphi_*). \quad (53)$$

From the values of $\tilde{F}_l(\theta, \varphi)$ and $\tilde{G}_l(\theta, \varphi)$ obtained above, λ and μ are computed as

$$\lambda = -\max\{\tilde{F}_l(\theta, \varphi), (\theta, \varphi) \in [0, \pi] \times [0, 2\pi[\}, \quad (54)$$

$$\mu = -\min\{\tilde{G}_l(\theta, \varphi), (\theta, \varphi) \in [0, \pi] \times [0, 2\pi[\}. \quad (55)$$

In doing so, the conditions (39) and (40) will automatically be satisfied. The value of the constants α_l and β_l are deduced from the above values of λ and μ via Eqs. (50) and (51). Finally the functions $F_l(\theta, \varphi)$ and $G_l(\theta, \varphi)$ are computed from Eqs. (48) and (49).

D. Compactification of the infinite domain

In the case where the external domain $\mathcal{D}_{\text{ext}} := \mathcal{D}_{\mathcal{N}-1}$ extends to infinity we introduce the mapping

$$[-1, 1] \times [0, \pi] \times [0, 2\pi[\rightarrow \mathcal{D}_{\text{ext}}, \quad (\xi, \theta', \varphi') \mapsto (r, \theta, \varphi), \quad (56)$$

in the form

$$u := 1/r = U(\xi, \theta', \varphi'), \quad (57)$$

$$\theta = \theta', \quad (58)$$

$$\varphi = \varphi', \quad (59)$$

where U is a smooth function which satisfies

$$U(-1, \theta, \varphi) = S_{\text{ext}}(\theta, \varphi)^{-1}, \quad (60)$$

$$U(+1, \theta, \varphi) = 0, \quad (61)$$

where $S_{\text{ext}}(\theta, \varphi) := S_{\mathcal{N}-2}(\theta, \varphi)$. The above two equations show that the inner boundary of \mathcal{D}_{ext} is defined by $\xi = -1$, whereas $\xi = +1$ corresponds to the infinity. We have already introduced such a compactification of the infinite domain in Ref. [9], in the case of a spherical inner boundary.

We choose the function $U(\xi, \theta, \varphi)$ as

$$U(\xi, \theta, \varphi) = \alpha_{\text{ext}}[\xi + A_{\text{ext}}(\xi)F_{\text{ext}}(\theta, \varphi) - 1], \quad (62)$$

where A_{ext} is the same polynomial of ξ as that defined in Eq. (35), and the constant α_{ext} and the function $F_{\text{ext}}(\theta, \varphi)$ are defined from the equations of the surface $S_{\mathcal{N}-2}$ by

$$\alpha_{\text{ext}}[-2 + F_{\text{ext}}(\theta, \varphi)] = S_{\text{ext}}(\theta, \varphi)^{-1}, \quad (63)$$

$$F_{\text{ext}}(\theta, \varphi) \leq 0. \quad (64)$$

The condition (64) ensures that $\partial U / \partial \xi \neq 0$, i.e., that the mapping (62) is not singular.

The equation for the inner boundary of the domain \mathcal{D}_{ext} being given, in the form of Eq. (1): $r = S_{\text{ext}}(\theta, \varphi)$, the procedure which leads to α_{ext} and $F_{\text{ext}}(\theta, \varphi)$, i.e. to the full determination of the function $U(\xi, \theta, \varphi)$, is the following one. First let us choose a point (θ_*, φ_*) on the surface S_{ext} . Equation (63) implies the following relation:

$$\alpha_{\text{ext}}[-2 + F_{\text{ext}}(\theta_*, \varphi_*)] = S_{\text{ext}}(\theta_*, \varphi_*)^{-1}. \quad (65)$$

By introducing the auxiliaries quantities

$$\lambda := \alpha_{\text{ext}} F_{\text{ext}}(\theta_*, \varphi_*), \quad (66)$$

$$\tilde{F}_{\text{ext}}(\theta, \varphi) := \alpha_{\text{ext}} F_{\text{ext}}(\theta, \varphi) - \lambda, \quad (67)$$

this equation translates as

$$-2\alpha_{\text{ext}} + \lambda = S_{\text{ext}}(\theta_*, \varphi_*)^{-1}, \quad (68)$$

whereas Eq. (63) becomes

$$\tilde{F}_{\text{ext}}(\theta, \varphi) = S_{\text{ext}}(\theta, \varphi)^{-1} - S_{\text{ext}}(\theta_*, \varphi_*)^{-1}. \quad (69)$$

From the above value of $\tilde{F}_{\text{ext}}(\theta, \varphi)$, λ is computed according to

$$\lambda = -\min\{\tilde{F}_{\text{ext}}(\theta, \varphi), (\theta, \varphi) \in [0, \pi] \times [0, 2\pi]\}. \quad (70)$$

In doing so, the condition (64) will automatically be satisfied (recall that $\alpha_{\text{ext}} < 0$). The value of α_{ext} is deduced from the above value of λ via Eq. (68). Finally the function $F_{\text{ext}}(\theta, \varphi)$ is computed from Eq. (67).

III. MULTIDOMAIN SPECTRAL METHOD

A. Spectral expansion of a physical field

The spirit of the multidomain spectral method is to perform spectral expansions on each domain \mathcal{D}_l , and with respect to the coordinates (ξ, θ, φ) instead of the physical coordinates (r, θ, φ) . We shall take as basis functions *separable* functions of (ξ, θ, φ) , i.e., functions that can be put under the form $X(\xi)\Theta(\theta)\Phi(\varphi)$. The variable φ being periodic, it is natural to use Fourier series in φ , i.e., to choose

$$\Phi_k(\varphi) = e^{ik\varphi} \quad -N_\varphi/2 \leq k \leq N_\varphi/2, \quad (71)$$

where N_φ is an even integer that we will call the number of degrees of freedom in φ . The associated collocation points (“grid points”) are

$$\varphi_k = 2\pi k/N_\varphi, \quad 0 \leq k \leq N_\varphi - 1. \quad (72)$$

Concerning $\Theta(\theta)$, one must use functions that are compatible with the expansion (10) of any regular scalar field f . We shall not use $\sin^{|m|} \theta P_{\ell-|m|}(\cos \theta)$, as suggested by Eq. (10), but a wider set, namely, the functions

$$\Theta_{kj}(\theta) = \cos(j\theta), \quad 0 \leq j \leq N_\theta - 1 \quad \text{for } m \text{ even}, \quad (73)$$

$$\Theta_{kj}(\theta) = \sin(j\theta), \quad 1 \leq j \leq N_\theta - 2 \quad \text{for } m \text{ odd}, \quad (74)$$

where N_θ is an integer that we will call the number of degrees of freedom in θ and m is the degree of the harmonic in the Fourier series with respect to φ : $m = k$ in the present case. The advantages of this choice are to allow the use of Fast-Fourier-Transform algorithms for computing the coefficients, as well as very simple matrices for the usual differential operators [26]. The associated collocation points are

$$\theta_j = \pi j / (N_\theta - 1), \quad 0 \leq j \leq N_\theta - 1. \quad (75)$$

Concerning the variable ξ , we also choose a set wider than merely $\xi^{\prime\prime}$: namely,

$$X_{kji}(\xi) = T_{2i}(\xi), \quad 0 \leq i \leq N_r - 1 \quad \text{for } j \text{ even}, \quad (76)$$

$$X_{kji}(\xi) = T_{2i+1}(\xi), \quad 0 \leq i \leq N_r - 2 \quad \text{for } j \text{ odd}, \quad (77)$$

where N_r is an integer that we will call the number of degrees of freedom in r and T_n denotes the n th degree Chebyshev polynomial. The associated collocation points are

$$\xi_i = \sin\left(\frac{\pi}{2} \frac{i}{N_r - 1}\right), \quad 0 \leq i \leq N_r - 1. \quad (78)$$

The above choice concerns the nucleus \mathcal{D}_0 only. For the intermediate and external domains, we choose instead

$$X_{kji}(\xi) = T_i(\xi), \quad (79)$$

along with the collocation points

$$\xi_i = -\cos[\pi i / (N_r - 1)], \quad 0 \leq i \leq N_r - 1. \quad (80)$$

Note that for the nucleus the above choice is the same as that presented in Ref. [27], once ξ is replaced by r . We refer the interested reader to that paper for a more detailed discussion about this choice (see also Appendixes A, B, and D of Ref. [18]).

When symmetry is present, we use different bases, in order to take the symmetry into account. For instance, an often existing symmetry is the symmetry with respect to the equatorial plane, i.e., the plane $\theta = \pi/2$. In this case, we use, instead of Eqs. (73), (74),

$$\Theta_{kj}(\theta) = \cos(2j\theta) \quad \text{for } m \text{ even}, \quad (81)$$

$$\Theta_{kj}(\theta) = \sin[(2j+1)\theta] \quad \text{for } m \text{ odd}. \quad (82)$$

The associated collocation points span only $[0, \pi/2]$, instead of $[0, \pi]$:

$$\theta_j = \frac{\pi}{2} \frac{j}{N_\theta - 1}, \quad 0 \leq j \leq N_\theta - 1. \quad (83)$$

Another usual symmetry is the above equatorial symmetry augmented by the symmetry under the transformation $\varphi \rightarrow \varphi + \pi$. This is the case of a triaxial ellipsoid, or of an axisymmetric star perturbed by even m modes. In this case, the φ -basis functions are

$$\Phi_k(\varphi) = e^{2ik\varphi}. \quad (84)$$

The associated collocation points span $[0, \pi[$, instead of $[0, 2\pi[$:

$$\varphi_k = \pi k / N_\varphi, \quad 0 \leq k \leq N_\varphi - 1. \quad (85)$$

The basis in θ become

$$\Theta_{kj}(\theta) = \cos(2j\theta), \quad (86)$$

instead of Eqs. (81), (82), the collocation points in θ remaining those given by Eq. (83). In this case, the basis for ξ in the nucleus contain only even polynomials:

$$X_{kji}(\xi) = T_{2i}(\xi), \quad (87)$$

the collocation points remaining the same as those given by Eq. (78).

B. Differential operators

In this section, we present how a first order differential operator, the gradient, and a second order one, the Laplacian, both applied to a scalar field, are expressed in terms of the coordinates system described above. The computation of any other kind of operator is straightforward.

The components of the gradient of a scalar field f in an orthonormal basis associated with the spherical coordinates (r, θ, φ) are

$$\frac{\partial f}{\partial r} = J_1^{-1} \frac{\partial f}{\partial \xi}, \quad (88)$$

$$\frac{1}{r} \frac{\partial f}{\partial \theta} = \frac{1}{R_l} \frac{\partial f}{\partial \theta'} - \frac{J_2}{J_1} \frac{\partial f}{\partial \xi}, \quad (89)$$

$$\frac{1}{r \sin \theta} \frac{\partial f}{\partial \varphi} = \frac{1}{R_l \sin \theta'} \frac{\partial f}{\partial \varphi'} - \frac{J_3}{J_1} \frac{\partial f}{\partial \xi}, \quad (90)$$

where the following abbreviations have been introduced:

$$J_1 := \frac{\partial R_l}{\partial \xi}, \quad (91)$$

$$J_2 := \frac{1}{R_l} \frac{\partial R_l}{\partial \theta'}, \quad (92)$$

$$J_3 := \frac{1}{R_l \sin \theta'} \frac{\partial R_l}{\partial \varphi'}. \quad (93)$$

Note that we have reintroduced the primes on θ and φ [cf. Eqs. (4), (5)] to avoid any confusion between the partial derivatives. The partial derivatives that appear in the quantities J_i are computed by (i) a (banded) matrix multiplication on the coefficients of the spectral expansion of the functions $F_l(\theta, \varphi)$ and $G_l(\theta, \varphi)$ and (ii) analytically for the polynomials $A_l(\xi)$ and $B_l(\xi)$. In the nucleus, J_2 is re-expressed as

$$J_2 = \frac{(3\xi^3 - 2\xi^5) \partial F_0 / \partial \theta' + (1/2)(5\xi^2 - 3\xi^4) \partial G_0 / \partial \theta'}{1 + (3\xi^3 - 2\xi^5) F_0 + (5\xi^2 - 3\xi^4) G_0}, \quad (94)$$

in order to avoid any division by a vanishing quantity at $\xi = 0$. The same thing is done for J_3 .

The above expressions are valid for the nucleus and the intermediate domains, i.e. for $l=0, \dots, \mathcal{N}-2$. For the compactified domain \mathcal{D}_{ext} , the quantity to be considered is $r^2 \nabla f$ instead ∇f . Indeed, gradients in the compactified domain are used in the computation of nonlinear terms in the relativistic gravitational field equations (scalar products of gradients of the metric potentials). We shall see below that the source of the Poisson equation on \mathcal{D}_{ext} is to be multiplied by r^4 , so that if each gradient is multiplied by r^2 , this multiplication by r^4 is automatically performed. The orthonormal components of $r^2 \nabla f$ on \mathcal{D}_{ext} are

$$r^2 \times \frac{\partial f}{\partial r} = - \left(\frac{\partial U}{\partial \xi} \right)^{-1} \frac{\partial f}{\partial \xi}, \quad (95)$$

$$r^2 \times \frac{1}{r} \frac{\partial f}{\partial \theta} = \frac{1}{U} \frac{\partial f}{\partial \theta'} - \left(\frac{\partial U}{\partial \xi} \right)^{-1} \frac{1}{U} \frac{\partial U}{\partial \theta'} \frac{\partial f}{\partial \xi}, \quad (96)$$

$$r^2 \times \frac{1}{r \sin \theta} \frac{\partial f}{\partial \varphi} = \frac{1}{U \sin \theta'} \frac{\partial f}{\partial \varphi'} - \left(\frac{\partial U}{\partial \xi} \right)^{-1} \frac{1}{U \sin \theta'} \frac{\partial U}{\partial \varphi'} \frac{\partial f}{\partial \xi}. \quad (97)$$

The Laplacian of a scalar field f reads

$$\begin{aligned} \Delta f = & J_1^{-1} \left\{ J_1^{-1} (1 + J_2^2 + J_3^2) \frac{\partial^2 f}{\partial \xi^2} + \frac{2}{R_l} \frac{\partial f}{\partial \xi} \right\} + \frac{1}{R_l^2} \Delta_{\theta\varphi} f \\ & - J_1^{-1} \left\{ 2 \left(\frac{J_2}{R_l} \frac{\partial^2 f}{\partial \theta \partial \xi} + \frac{J_3}{R_l \sin \theta} \frac{\partial^2 f}{\partial \varphi \partial \xi} \right) + \left[\frac{1}{R_l^2} \Delta_{\theta\varphi} R_l \right. \right. \\ & \left. \left. + J_1^{-1} \left(J_1^{-1} (1 + J_2^2 + J_3^2) \frac{\partial^2 R_l}{\partial \xi^2} - 2 \left(\frac{J_2}{R_l} \frac{\partial^2 R_l}{\partial \theta \partial \xi} \right. \right. \right. \right. \\ & \left. \left. \left. + \frac{J_3}{R_l \sin \theta} \frac{\partial^2 R_l}{\partial \varphi \partial \xi} \right) \right] \frac{\partial f}{\partial \xi} \right\}, \quad (98) \end{aligned}$$

where the primes on θ and φ have been abandoned again and the following abbreviation has been introduced:

$$\Delta_{\theta\varphi} := \frac{\partial^2}{\partial \theta^2} + \frac{1}{\tan \theta} \frac{\partial}{\partial \theta} + \frac{1}{\sin^2 \theta} \frac{\partial^2}{\partial \varphi^2}. \quad (99)$$

C. Resolution of the Poisson equation

For many astrophysical applications, one has to solve the Poisson-like equation

$$\Delta f = \sigma(f), \quad (100)$$

for some ‘‘potential’’ f . Note that for relativistic computations, $\sigma(f)$ is not compactly supported (see, e.g., Ref. [9]) and generally decreases as $1/r^4$ when $r \rightarrow +\infty$.

When expressed in terms of the variables (ξ, θ, φ) , the Laplacian takes the complicated form (98), for which it is not obvious to find eigenfunctions. Therefore, we introduce, in each domain \mathcal{D}_l , a new radial coordinate

$$\zeta := \alpha_l \xi + \beta_l, \quad (101)$$

where α_l and β_l are the same constants as in Eqs. (11) and (34) (in the nucleus: $\beta_0=0$). In the exterior domain, we introduce

$$\eta := \alpha_{\text{ext}}(\xi - 1), \quad (102)$$

where α_{ext} is the same constant as in Eq. (62). We may then split the Laplacian operator Δ into a pseudo-Laplacian $\tilde{\Delta}$ and a part which would vanish if the domains \mathcal{D}_l were exactly spherical (in this case, the coordinates ζ and η introduced here above would coincide with the physical coordinates r and $u=1/r$ respectively). By pseudo-Laplacian, we mean the operator which once expressed in terms of (ζ, θ, φ) has the same structure than the Laplacian operator in spherical coordinates:

$$\tilde{\Delta} := \frac{\partial^2}{\partial \zeta^2} + \frac{2}{\zeta} \frac{\partial}{\partial \zeta} + \frac{1}{\zeta^2} \Delta_{\theta\varphi}, \quad (103)$$

where $\Delta_{\theta\varphi}$ is defined by Eq. (99). In the exterior domain, the pseudo-Laplacian is defined instead by

$$\tilde{\Delta} := \frac{\partial^2}{\partial \eta^2} + \frac{1}{\eta^2} \Delta_{\theta\varphi}. \quad (104)$$

It is much easier to invert the operator $\tilde{\Delta}$ than the operator Δ : using spherical harmonics in (θ, φ) , the problem reduces to a system of second order ordinary differential equations with respect to the variable ζ . Moreover, the junction conditions between the various domains are easily imposed, as explained below.

The Poisson equation (100) becomes

$$a \tilde{\Delta} f = \sigma(f) + \mathcal{R}(f), \quad (105)$$

where

$$a := \alpha_l^2 J_1^{-2} (1 + J_2^2 + J_3^2), \quad (106)$$

$$\begin{aligned} \mathcal{R}(f) := & \left[J_1^{-1} \frac{R_l}{\xi + \beta_l / \alpha_l} (1 + J_2^2 + J_3^2) - 1 \right] \frac{2}{J_1 R_l} \frac{\partial f}{\partial \xi} \\ & + \left[J_1^{-2} \frac{R_l^2}{(\xi + \beta_l / \alpha_l)^2} (1 + J_2^2 + J_3^2) - 1 \right] \frac{1}{R_l^2} \Delta_{\theta\varphi} f \\ & + J_1^{-1} \left\{ 2 \left(\frac{J_2}{R_l} \frac{\partial^2 f}{\partial \theta \partial \xi} + \frac{J_3}{R_l \sin \theta} \frac{\partial^2 f}{\partial \varphi \partial \xi} \right) \right. \\ & + \left[\frac{1}{R_l^2} \Delta_{\theta\varphi} R_l + J_1^{-1} \left(J_1^{-1} (1 + J_2^2 + J_3^2) \frac{\partial^2 R_l}{\partial \xi^2} \right. \right. \\ & \left. \left. - 2 \left(\frac{J_2}{R_l} \frac{\partial^2 R_l}{\partial \theta \partial \xi} + \frac{J_3}{R_l \sin \theta} \frac{\partial^2 R_l}{\partial \varphi \partial \xi} \right) \right) \right] \frac{\partial f}{\partial \xi} \left. \right\}. \quad (107) \end{aligned}$$

In order to let appear only the operator $\tilde{\Delta}$ in the left-hand side of Eq. (105), we introduce

$$a_l := \max_{\mathcal{D}_l} a, \quad (108)$$

and recast Eq. (105) into

$$\tilde{\Delta} f = \frac{1}{a_l} [\sigma(f) + \mathcal{R}(f) + (a_l - a) \tilde{\Delta} f]. \quad (109)$$

Since f appears on the right-hand side of this equation, we solve it by iteration. In addition, we introduce some relaxation in the computation of the term $\tilde{\Delta} f$ in the right-hand side of Eq. (109). More specifically, we solve at each step of the iterative scheme the equation

$$\tilde{\Delta} f^{J+1} = \tilde{\sigma}^J, \quad (110)$$

where the index J denotes the step at which the quantities are taken and $\tilde{\sigma}^J$ is the following source, computed from the value of f at the step J :

$$\tilde{\sigma}^J = a_l^{-1} \{ \sigma(f^J) + \mathcal{R}(f^J) + (a_l - a) [\lambda \tilde{\sigma}^{J-1} + (1 - \lambda) \tilde{\sigma}^{J-2}] \}. \quad (111)$$

In this expression, λ is a relaxation parameter (a typical value is $\lambda=1/2$) and $\mathcal{R}(f^J)$ is to be computed according to Eq. (107). For the first step ($J=0$), f^J , $\tilde{\sigma}^{J-1}$, and $\tilde{\sigma}^{J-2}$ are set to zero or to their value at a previous step in an evolutionary scheme.

We have exposed the method of resolution of Eq. (110) elsewhere [27,9]. Let us simply mention that we first perform a transformation from the bases in (θ, φ) described in Sec. III A (Chebyshev polynomials in $\cos \theta$, Fourier expansion in φ) to spherical harmonics $Y_{\ell}^m(\theta, \varphi)$, by means of a matrix multiplication onto the coefficients of the θ expansion. For each value of (ℓ, m) , Eq. (110) gives then a second order ordinary differential equation with respect to ζ , the solution of which amounts to inverting a banded matrix. Two solutions of the homogeneous equation ($\Delta f=0$) are then added

in order to connect the solution and its first derivative across the boundaries between the \mathcal{N} domains. More precisely, the global boundary condition, generally $f \rightarrow 0$ when $r \rightarrow +\infty$, is imposed by setting the value of f at the exterior boundary of the external domain, which is exactly $r = +\infty$ as explained in Sec. II D. The matching between the various domains amounts then to the resolution of a simple system of $2\mathcal{N} - 1$ linear equations for the coefficients of the homogeneous solutions to be added in each domain. Note that this matching is performed for each value of (ℓ, m) .

IV. REGULARIZATION OF THE SOURCE OF POISSON EQUATION

A. Description of the method

The analytical properties of the source of the gravitational field at the boundary of the star depend on the equation of state (EOS). For a polytrope of adiabatic index γ ($P \propto n^\gamma$), the matter density n behaves as $H^{1/(\gamma-1)}$ where H is the specific enthalpy. Consequently, for $\gamma > 2$, the derivative dn/dH has an infinite value for $H=0$, i.e., at the surface of the star and dn/dr diverges at surface of the star. For values of $\gamma < 2$ only derivatives of higher order diverge (actually there exists some value of γ , e.g., $\gamma=4/3$, for which all derivatives vanish or have a finite value at the surface of the star).

In a steady state configuration H is Taylor expandable at the neighborhood of the star's surface [this can be easily seen on Eq. (123) below]. Therefore H vanishes as $r - R(\theta, \varphi)$, where $R(\theta, \varphi)$ is the equation of the star's surface and n behaves as $n \sim [r - R(\theta, \varphi)]^{1/(\gamma-1)}$ (this analysis remains valid even for EOS more general than the polytropic one if γ is defined as $\gamma = d \ln(P)/d \ln(H)|_{H=0}$). Consequently n is generally not a \mathcal{C}^∞ function. This singular behavior implies that the \mathcal{L}^2 truncation error of the spectral approximation is no more evanescent and moreover that Gibbs phenomenon is present. This fact is especially awkward when studying the stability of equilibrium configurations or looking for bifurcation points because high accuracy is required. In practice γ cannot be larger than 3 [16,17]. Note that in the literature the potential in spherical coordinates is often computed by expanding the source in spherical harmonics $Y_l^m(\theta, \varphi)$ and by computing the radial part with a finite difference method. In this case the Gibbs phenomenon will appear in the angular part of the solution. The situation is even worse if the radial part of the potential is computed with a spectral method. A method to recover spectral accuracy in such cases is as follows.

We first introduce a known potential Φ_{div} such that $n_{\text{div}} := \Delta \Phi_{\text{div}}$ has the same pathological behavior as n and such that $n - n_{\text{div}}$ is a regular function (at least more regular than n) and numerically solve

$$\Delta \Phi_{\text{regu}} = n - n_{\text{div}}, \quad (112)$$

where $\Phi_{\text{regu}} := \Phi - \Phi_{\text{div}}$. Consider, for instance,

$$\Phi_{\text{div}} = F(\xi, \theta, \varphi)(1 - \xi^2)^{(\alpha+2)}, \quad (113)$$

where $\alpha = 1/(\gamma - 1)$, F is an arbitrary regular function and ξ is a new radial variable such that $\xi = 1$ at the surface of the star (see Sec. II). It is easy to see that $\Delta \Phi_{\text{div}}$ has a term vanishing at the surface as $(1 - \xi)^\alpha$ (i.e., with the same pathological behavior as n). We have indeed

$$\begin{aligned} \tilde{\Delta} \Phi_{\text{div}} &= \tilde{\Delta} F \xi^2 (1 - \xi^2)^{(\alpha+2)} \\ &\quad - 4(\alpha + 2) \xi (1 - \xi^2)^{(\alpha+1)} \partial_\xi F \\ &\quad + (\alpha + 2) [-6(1 - \xi^2)^{(\alpha+1)} \\ &\quad + 4(\alpha + 1) \xi^2 (1 - \xi^2)^\alpha] F, \end{aligned} \quad (114)$$

where $\tilde{\Delta}$ is the Laplacian computed with respect to (ξ, θ, φ) [cf. Eq. (103)].

The choice of the factor of $(1 - \xi)^{(\alpha+2)}$ is done in order that Φ_{div} has the required regularity properties at $\xi = 0$ and the required behavior at the boundary of the star. The choice of $F(\xi, \theta, \varphi)$ is arbitrary. If we choose for $F(\xi, \theta, \varphi)$ an harmonic function, $\tilde{\Delta} F = 0$, the first term of the right-hand side of Eq. (114) vanishes. This is an advantage because this term can be quite large and, consequently, give rise to a large error in computing Φ_{regu} . We write $\Phi_{\text{div}} = \sum_{l,m} a_{lm} \Phi_{lm}$, where

$$\Phi_{lm} := \xi^l (1 - \xi^2)^{(\alpha+2)} Y_l^m(\theta, \varphi) \quad (115)$$

and where a_{lm} are some numerical coefficients to be determined. We then obtain $n_{\text{div}}(\xi, \theta, \varphi) = \sum_{l,m} a_{lm} C_l(\xi) Y_l^m(\theta, \varphi)$, with

$$\begin{aligned} C_l(\xi) &:= (\alpha + 2) [- (4l + 6) (1 - \xi^2)^{(\alpha+1)} \xi^l \\ &\quad + 4(\alpha + 1) \xi^{l+2} (1 - \xi^2)^\alpha]. \end{aligned} \quad (116)$$

We now have to determine the values of the coefficients a_{lm} which give the most regular function $n_{\text{regu}} := n - n_{\text{div}}$. The criterion which seems to give the best results is the following one. We expand n and n_{div} as truncated series of spherical harmonics $Y_l^m(\theta, \varphi)$ and Chebyshev polynomial $T_i(\xi)$

$$n(\xi, \theta, \varphi) = \sum_{i,l,m=0}^{I,L,M} n_{ilm} T_i(\xi) Y_l^m(\theta, \varphi) \quad (117)$$

and each of the functions $C_l(\xi)$ in a Chebyshev series

$$C_l(\xi) = \sum_i^I C_{li} T_i(\xi). \quad (118)$$

The value of a_{lm} is computed in such a way that the l th coefficient of the truncated series of n_{regu} vanishes:

$$a_{lm} = n_{ilm} / C_{ll}. \quad (119)$$

By means of the above procedure, we eliminate in n the pathological term vanishing as $(1 - \xi)^\alpha$ but we introduce an-

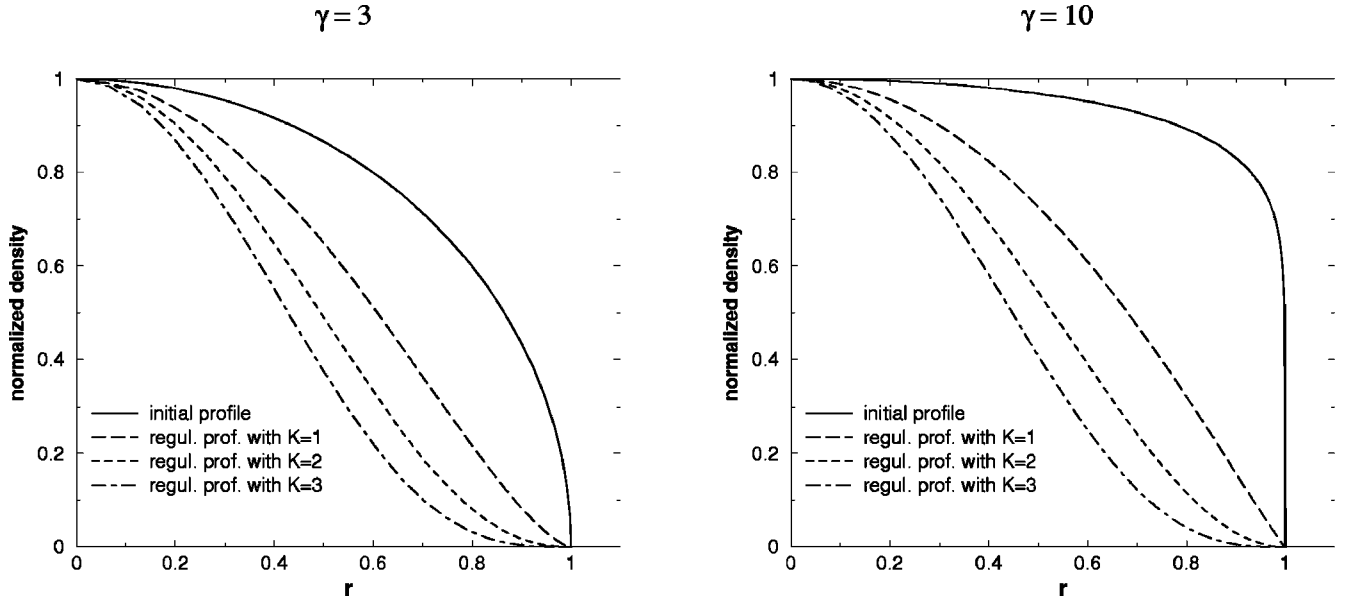


FIG. 2. Original and regularized density profiles for $\gamma=3$ and $\gamma=10$ polytropes. The regularized profiles are rescaled to take the value 1 at the origin.

other pathological term $\propto(1-\xi^2)^{\alpha+1}$. However, the divergence occurs in a higher order derivative of this term so that it has a much weaker effect on the accuracy of the result. The method can be improved by taking

$$\Phi_{\text{div}} = F(\xi, \theta, \varphi)(1-\xi^2)^{\alpha+2} [a_1 + a_2(1-\xi^2) + a_3(1-\xi^2)^2 + \dots + a_K(1-\xi^2)^{K-1}] \quad (120)$$

instead of Eq. (113). The coefficients a_k are chosen in such a way that the first, second, \dots , K th derivatives of n_{regu} vanish at $\xi=1$. Let us call K the regularization degree of the procedure.

Note that, since Φ_{div} and $\partial_\xi \Phi_{\text{div}}$ vanish at the surface of the star, the boundary condition one has to impose to solve $\Delta \Phi_{\text{regu}} = n_{\text{regu}}$ is the same as that for $\Delta \Phi = n$. We want to point out that the above regularization technique can be used *mutatis mutandis* also when a finite difference method is used.

B. Examples

Consider two polytropic EOS of adiabatic index $\gamma=3$ and $\gamma=10$ with a spherically symmetric distribution of the enthalpy $H=1-\xi^2$. The corresponding source density are $n_3(\xi)=(1-\xi^2)^{1/2}$ and $n_{10}(\xi)=(1-\xi^2)^{1/9}$. Figure 2 shows the mass distributions n and n_{regu} for various values of the regularization degree K [Eq. (120)]. Note that in the case of $\gamma=10$ the procedure improves considerably the behavior of the source n_{regu} even for $K=1$.

The method can be tested in the case of $\gamma=3$ by direct comparison with the analytical solution. In this case the gravitational field $G=\partial_r \Phi$ reads

$$G = \frac{1}{r^2} \int_0^r (1-u^2)^{1/2} u^2 du$$

$$= \frac{1}{8r^2} [\arcsin r + r(1-r^2)^{1/2} - 2r(1-r^2)^{3/2}]. \quad (121)$$

Figure 3 shows the relative \mathcal{L}^1 error ϵ on G as a function of the number of degrees of freedom N_r . The error ϵ follows approximately a power law $\epsilon \propto N_r^{-\beta}$. The dependence of the exponent β with respect to the regularization degree K is shown in Fig. 4. A value as high as $\beta \approx 17$ can be achieved with only $K=6$. Note that the relation $\epsilon = N_r^{-\beta}$ is only an approximate law. This means that the error tends to become evanescent when the regularization degree increases.

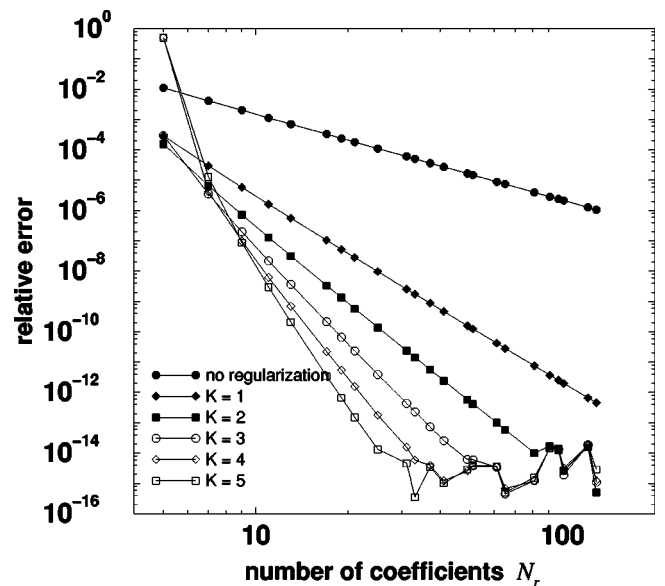


FIG. 3. Relative \mathcal{L}^1 error ϵ on the gravitational field as a function of the number of degrees of freedom N_r for different regularization degrees K .

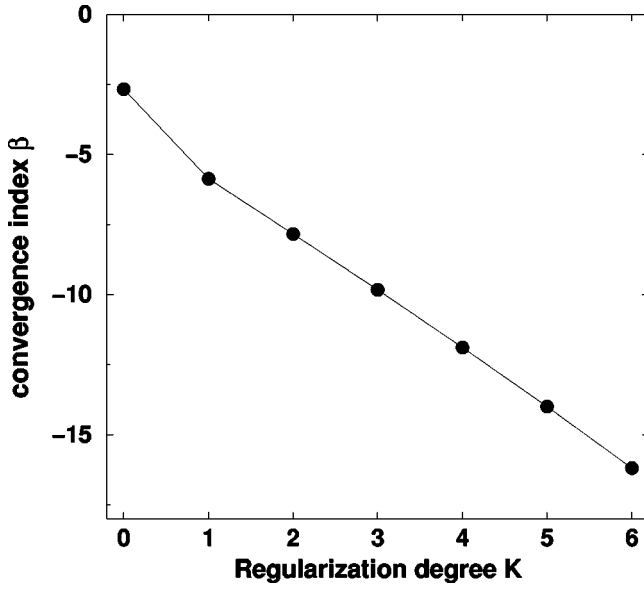


FIG. 4. Dependence of the exponent β on the regularization degree K .

V. ILLUSTRATIVE APPLICATIONS

A. 3D stationary configurations

In this section, we sketch the general structure of a code for computing single star stationary configurations under the influence of rotation and a tidal potential. For simplicity we present only the Newtonian case, the relativistic one showing no new qualitative feature but simply involving more equations.

The equilibrium configuration of a cold star rotating rigidly at the angular velocity Ω with respect to some inertial frame and embedded in a tidal potential Φ_{tide} is governed by the following three equations:¹

$$\Delta \Phi_{\text{grav}} = 4\pi G \rho, \quad (122)$$

$$H + \Phi_{\text{grav}} - \frac{1}{2}(\Omega r \sin \theta)^2 + \Phi_{\text{tide}} = \text{const}, \quad (123)$$

$$\rho = \rho(H). \quad (124)$$

Equation (122) is the Poisson equation linking the gravitational potential Φ_{grav} to the mass density ρ . Equation (123) is the first integral which can be derived from the Euler equation governing the (perfect) fluid velocity under the stationarity assumption; this equation relates the specific enthalpy of the fluid H to the internal and external potentials. Finally Eq. (124) is the matter equation of state in the zero-temperature approximation.

The number of domains used for solving this problem is $\mathcal{N}=3$: one domain \mathcal{D}_0 for the star (the nucleus, cf. Sec. II B), one intermediate domain \mathcal{D}_1 (cf. Sec. II C), the outer

boundary of which is spherical and the external domain \mathcal{D}_2 (cf. Sec. II D). In fact, if one treats only the Newtonian case, one domain would be sufficient (i.e., the nucleus) because Eq. (122) has a compact support, which is no longer true in the relativistic case.

A solution is specified by the central value of H (or ρ), H_c say, the value of Ω and the expression of Φ_{tide} . These quantities being given, the iterative method of resolution is as follows. The \mathcal{N} domains are first taken to be exactly spherical. One starts from a very crude density profile, for instance, $\rho = \text{const}$ in \mathcal{D}_0 . Solving the Poisson equation (122) by means of the method presented in Sec. III C leads to the gravitational potential Φ_{grav} . Inserting its value into Eq. (123) gives a new profile for the specific enthalpy H [the constant on the right-hand side of Eq. (123) is fully determined by the requirement that $H = H_c$ at the center of the star]. The surface of the star being defined by $H = 0$, its equation $r = S_0(\theta, \varphi)$ [using the notation of Eq. (1)] is found by searching for the equipotential $H = 0$ in the newly determined H field. This defines a new domain \mathcal{D}_0 . The corresponding mapping $R_0(\xi, \theta, \varphi)$, i.e., the value of the constant α_0 and the functions $F_0(\theta, \varphi)$ and $G_0(\theta, \varphi)$ [cf. Eq. (11)] is computed according to the procedure described in Sec. II B. The new intermediate domain \mathcal{D}_1 is defined by the new inner boundary \mathcal{S}_0 (the surface of the star) and the unchanged spherical outer boundary \mathcal{S}_1 . The corresponding mapping $R_1(\xi, \theta, \varphi)$ is computed according to the procedure described in Sec. II C. The external domain \mathcal{D}_2 remains unchanged.

The physical location (r, θ, φ) of the collocation points $(l, \xi_i, \theta_j, \varphi_k)$ (where l is the domain index) corresponding to these new mappings is *a priori* different than that of the previous mappings, where all the fields were known. Therefore, one has to compute the values of the fields at the new collocation points. In the present case, it is sufficient to do so only for the specific enthalpy H . In domain l , the collocation point $(\xi_i, \theta_j, \varphi_k)$ has the physical radial coordinate

$$r = R_l^J(\xi_i, \theta_j, \varphi_k), \quad (125)$$

where the superscript J refers to the step in the iterative procedure: $R_l^J(\xi, \theta, \varphi)$ is the current value of the mapping of the domain \mathcal{D}_l , whereas $R_l^{J-1}(\xi, \theta, \varphi)$ is the previous value. Let us denote the inverse mapping at the previous step by $[L^{J-1}(r, \theta, \varphi), \Xi^{J-1}(r, \theta, \varphi)]$. This inverse mapping is computed by searching for the zero of the function $(l, \xi) \mapsto r - R_l(\xi, \theta, \varphi)$. The values of H at the collocation points of the new mapping are given by

$$\begin{aligned} H^J(l, \xi_i, \theta_j, \varphi_k) \\ = H^{J-1}[L^{J-1}(r^J, \theta_j, \varphi_k), \Xi^{J-1}(r^J, \theta_j, \varphi_k), \theta_j, \varphi_k], \end{aligned} \quad (126)$$

where $r^J := R_l^J(\xi_i, \theta_j, \varphi_k)$. The value of H on the right-hand side is to be taken at a point which *a priori* does not coincide with a collocation point in ξ . It is computed by a direct

¹See Ref. [28] for a discussion of these equations, including the relativistic case.

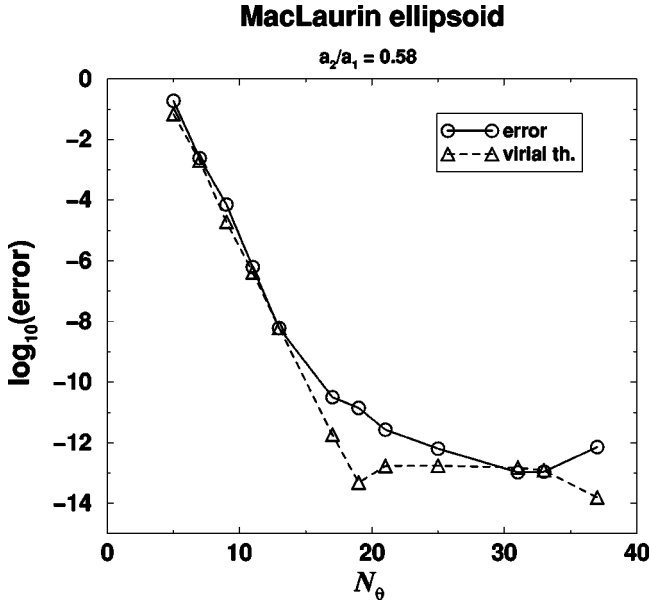


FIG. 5. Logarithm of the relative error of the numerical solution with respect to the number of degrees of freedom in θ for a MacLaurin spheroid at the Jacobi-Dedekind bifurcation point (the number of degrees of freedom in r is $N_r = 2N_\theta - 1$). Also shown is the error in the verification of the virial theorem.

summation, by means the spectral expansion of H . Using the notations of Sec. III A, it is written as

$$H(l, \xi, \theta, \varphi) = \sum_{k=0}^{N_\varphi-1} \left[\sum_{j=0}^{N_\theta-1} \left(\sum_{i=0}^{N_r-1} \hat{H}_{lkji} X_{kji}(\xi) \right) \Theta_{kj}(\theta) \right] \Phi_k(\varphi), \quad (127)$$

where \hat{H}_{lkji} are the coefficients of H in domain l . Note that from the computational point of view, this summation is the most expensive operation of the method: it scales indeed as $(N_r N_\theta N_\varphi)^2$. It may be possible to replace the whole summation (127) by a truncated one or by some interpolation from the values of H at the collocation points, in order to reduce the computational cost. The main advantage of the summation (127) is that it does not introduce any additional error in the method: the right-hand side of Eq. (127) is the value of H at the specified point within spectral accuracy.

Once H is computed at the collocation points of the new mapping by means of Eq. (126), the equation of state (124) is used to find the values of the mass density ρ at the collocation points. A new iteration may then begin.

In all the computations we have made, we have found that this procedure converges. For stationary rotating stars in general relativity, a rigorous proof of the convergence of such iterative method (except for the remapping of the physical space at each step) has been given by Schaudt and Pfister [29].

B. MacLaurin ellipsoids

The multidomain spectral method can handle constant density (incompressible matter) rotating bodies without any

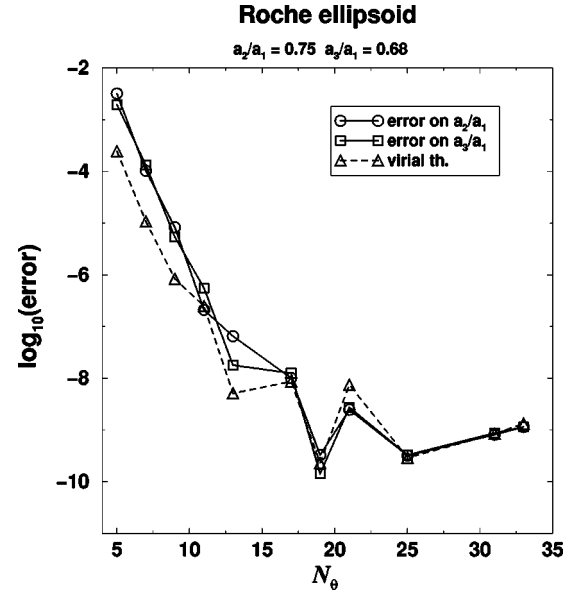


FIG. 6. Logarithm of the relative global error of the numerical solution with respect to the number of degrees of freedom in θ for a Roche ellipsoid for an equal mass binary system and $\Omega^2/(\pi G \rho) = 0.1147$ (the numbers of degrees of freedom in the other directions are $N_r = 2N_\theta - 1$ and $N_\varphi = N_\theta - 1$). Also shown is the error in the verification of the virial theorem.

Gibbs phenomenon. With classical spectral methods, the Gibbs phenomenon would have been very severe since the density itself, and not some of its derivatives, is discontinuous across the stellar surface for incompressible fluids. This gives us the opportunity to quantify the accuracy of the method since exact analytical solutions are known for incompressible bodies: the so-called ellipsoidal figures of equilibrium (see, e.g., Ref. [30]). Note that an ellipsoid is not a particular case for the mapping (11): all the coefficients of the expansion of $F_0(\theta, \varphi)$ and $G_0(\theta, \varphi)$ with the bases described in Sec. III A are nonzero. In this respect, the ellipsoidal figures constitute a strong test of the method.

For single rigidly rotating objects in the Newtonian regime, the more simple ellipsoidal solutions are constituted by the family of MacLaurin spheroids, which are axisymmetric about their rotation axis. We have computed them by means of the procedure presented in Sec. V A, setting $\Phi_{\text{tide}} = 0$ and the equation of state (124) to be simply $\rho = \text{const}$. The axisymmetry allows us to employ $N_\varphi = 1$. The code converges towards ellipsoidal configurations and we measure the error by comparing the eccentricity $e := \sqrt{1 - (r_p/r_{\text{eq}})^2}$ (where r_p and r_{eq} are, respectively, the polar and equatorial radii) of the numerical solution with that of the analytical solution. The result of this comparison is presented in Fig. 5 for a MacLaurin spheroid located on the MacLaurin sequence at the point where the Jacobi and Dedekind sequences branch off: the eccentricity is $e = 0.8127$, which corresponds to the ratio $r_p/r_{\text{eq}} = 0.5827$. Shown in Fig. 5 is the relative error on the eccentricity as a function of the number of coefficients in the θ expansion. For these calculations, the number of coefficients in the ξ expansion in each domain is $N_r = 2N_\theta - 1$. The straight line behavior of the left side of Fig. 5 shows that

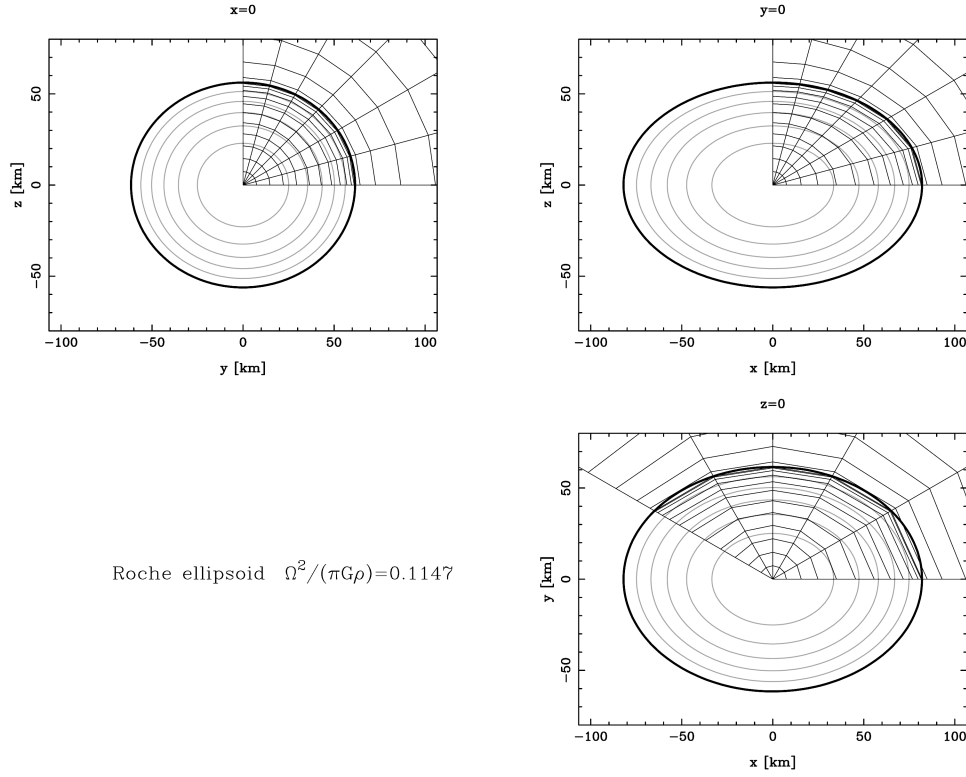


FIG. 7. Orthogonal plane sections in the numerical solution obtained for the Roche ellipsoid represented by the second set of points starting from the left on Fig. 6 (i.e., corresponding to $N_r = 13$, $N_\theta = 7$, and $N_\varphi = 6$). Shown are the isoenthalpy lines, as well as the numerical grid. This computation took a few seconds on a R4400/150 MHz processor.

the error is evanescent, i.e., that it decreases as $\exp(-N_\theta)$. For $N_\theta \geq 20$, the error saturates at the level of $10^{-12} - 10^{-11}$. This is due to the round-off errors in the computation, which is performed with a 15-digit accuracy. It is instructive to compare this result with that obtained with a classical spectral method, i.e., with fixed spherical domains, as exposed in Ref. [9]. For instance, Fig. 5 can be directly compared with Fig. 7 of Ref. [9]: this latter shows a power-law error decay only (of type $N_\theta^{-4.5}$), due to the Gibbs phenomenon at the star's surface. Moreover, the error saturates at the level of 10^{-5} . Note that this result was obtained with a polytropic equation of state (adiabatic index $\gamma = 2$), for which the density is continuous across the surface of star; the fixed-spherical-domain spectral method presented in Ref. [9] was not able to treat incompressible fluid.

Also shown in Fig. 5 is the relative accuracy with which the 3D virial theorem is satisfied. The 3D Newtonian virial theorem² states that for a stationary configuration $2T + 3P + W = 0$, where T is the total kinetic energy (with respect to the inertial frame), P is the integral of the pressure throughout the star and W is the gravitational potential energy. We have computed each of these three integrals for the numerical solution and evaluated the quantity

$$\varepsilon := \left| 1 - \frac{2T + 3P}{|W|} \right|. \quad (128)$$

For an exact solution, $\varepsilon = 0$. The triangles plotted in Fig. 5 depict the value of $\log_{10}\varepsilon$ for the numerical models. Figure 5 shows that the virial error is very well correlated with the error evaluated by a direct comparison with the analytical solution. This gives us a great deal of confidence when using the virial error to evaluate the numerical error in more general cases, when no analytical solution is available.

C. Roche ellipsoids

Roche ellipsoids are equilibrium solutions for incompressible fluid bodies in a synchronized binary system, within the approximation of taking only the second order term in the expansion (around the center of mass of one star) of the gravitational potential of the companion. They are obtained by setting

$$\Phi_{\text{tide}} = -\frac{GM_{\text{comp}}}{|a|} \left(1 + \frac{x}{a} + \frac{2x^2 - y^2 - z^2}{a^2} \right) \quad (129)$$

in Eq. (123), where a is the abscissa of the center of mass of the companion in the Cartesian frame (x, y, z) centered at the center of mass of the star under consideration. Note that in Eq. (123), r must now be the distance to the center of mass of the binary system and θ the angle with respect to the

²As opposed to the 2D virial identity, see Refs. [31] and [32] for a discussion.

TABLE I. CPU time cost on a R4400/150MHz processor as a function of the number of degrees of freedom for the calculation of the Roche ellipsoid configuration corresponding to Fig. 6. The iteration is halted when the relative discrepancy between two successive steps reaches 10^{-13} .

N_r	N_θ	N_φ	No. of steps	CPU time per step (s)
25	13	12	116	6.92
33	17	16	107	24.2
49	25	24	115	189.16
65	33	32	106	861.6

rotation axis of the system. Moreover, Ω must be chosen so that $\Omega^2 = G(M + M_{\text{comp}})/a^3$, in order that the linear term in x which appears in Eq. (123) vanishes and one is left with an ellipsoidal solution.

The analytical solutions for Roche ellipsoid are given in the classic book by Chandrasekhar [30]. However, they are given with an accuracy of five digits only (Table XVI in Ref. [30]), which is not sufficient for our comparison project: the accuracy achieved by the numerical code is far better than 10^{-5} as we shall see below. Therefore, we have written a small MATHEMATICA [33] program to compute Chandrasekhar's "index symbols" A_1 , A_2 , and A_3 and obtain Roche solutions with an arbitrary number of digits.

Figure 6 presents the results of the comparison between the numerical solution obtained by means of the method described in Sec. V A and the analytical solution. Let us recall that ellipsoidal shapes are not privileged in our formalism, so that this type of comparison constitute a strong test of our method. The comparison is conducted at fixed values of Ω/ρ and the mass ratio M_{comp}/M . Two global errors can then be defined: (i) the error on the axis ratio a_2/a_1 and (ii) the error on the axis ratio a_3/a_1 , a_1 being the major axis of the triaxial ellipsoid (directed along the line of the two centers of mass), a_2 being the orthogonal axis in the orbital plane, and a_3 being the axis perpendicular to the orbital plane. These two errors are shown in Fig. 6 for a Roche ellipsoid with $\Omega^2/(\pi G\rho) = 0.1147$ and $M_{\text{comp}}/M = 1$. The corresponding axis ratios are $a_2/a_1 = 0.7506$ and $a_3/a_1 = 0.6853$. The numerical solution is depicted in Fig. 7 by three plane sections obtained with the following (small) numbers of coefficients: $N_r = 13$, $N_\theta = 7$, and $N_\varphi = 6$. Also show in this figure is the numerical grid (collocation points) used in the problem (only the domain \mathcal{D}_0 and a part of \mathcal{D}_1 are represented in the figure). Even with such a small number of points, the relative error is of order 1×10^{-4} (cf. Fig. 6). This explains why despite the fact that the numerical grid is quite coarse, the isenthalpy surfaces shown in Fig. 7 are so smooth.

Figure 6 gives the two global errors as a function of the number of coefficients in the θ expansions N_θ . The number of coefficients employed in the other directions are $N_r = 2N_\theta - 1$ and $N_\varphi = N_\theta - 1$. As in Fig. 5, the exponential decay of the error for $N_\theta \leq 13$ means that the error is evanescent. For $N_\theta \geq 19$, the error saturates at the level of a few 10^{-10} due to the round-off errors in the computation, this

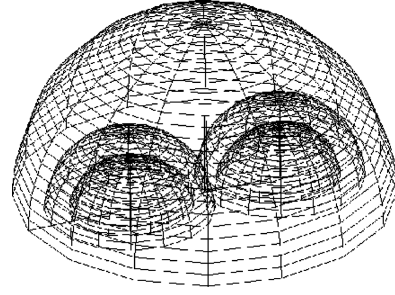


FIG. 8. Representation of the numerical domains that we use to compute relativistic steady-state configurations of binary neutron stars systems. The external domain extends to spatial infinity in order to compute the exact gravitational potentials. Due to the symmetry of the problem, only the $z > 0$ part of space is taken into account.

latter being performed with a 15-digit accuracy. The cost in CPU time for different numbers of degrees of freedom is shown in Table I.

Also shown in Fig. 6 is the relative accuracy with which the 3D virial theorem is satisfied. This error estimator is defined in the same way as in Sec. V B. As in the axisymmetric case (MacLaurin ellipsoids), we find a high correlation between the virial error and the errors obtained by direct comparison with the analytical solution.

VI. CONCLUSION AND PERSPECTIVES

We have presented a new numerical approach capable of handling the surface discontinuities of stellar configurations, provided these discontinuities are starlike, which covers a wide range of astrophysically relevant situations. When used along with spectral methods this adaptive-domain technique ensures that no Gibbs phenomenon can appear. This results in a very high precision (evanescent error), as demonstrated in Sec. V by a comparison with exact analytical solutions. The relative error for 3D configurations can reach 10^{-10} with a relatively small number of degrees of freedom ($N_r \times N_\theta \times N_\varphi = 37 \times 19 \times 18$ in each domain). Let us recall that very high accuracy is required for a lot of astrophysical problems such as numerical stability analysis. Among these problems let us mention the study of symmetry breaking of rapidly rotating stars and the determination of the orbital frequency of the last stable orbit of a neutron stars binary system.

The multidomain spectral method is particularly well adapted to the computation of relativistic binary neutron star system. Three sets of domains can be used in this problem (see Fig. 8): two sets of (three or more) domains centered on each star and a third set of (two or more) domains centered at the intersection between the rotation axis and the orbital plane. This latter set of domains which reaches spatial infinity is required to compute the gravitational field of relativistic configurations. When needed, the quantities computed on one of the three domain sets are evaluated at the collocation points of another set by means of the method presented in Sec. V A. We are currently applying this numerical method to the computation of steady-state configurations of relativistic counter-rotating (i.e., irrotational with respect to an in-

ertial frame) neutron star binaries, following the formulation developed in Ref. [1]. We will report on the astrophysical results in a forthcoming paper.

An interesting by-product of the present technical paper is as follows. In a previous work [9], we were able to demonstrate that the virial error is representative of the true error

(measured by direct comparison with analytical solutions) only in the spherically symmetric case. We had inferred that this remains valid in the axisymmetric and 3D cases. In the present work, we have confirmed this conjecture, thanks to the ability of the present method to treat incompressible fluids, for which 3D analytical solutions are available.

-
- [1] S. Bonazzola, E. Gourgoulhon, and J-A. Marck, *Phys. Rev. D* **56**, 7740 (1997).
- [2] S. Bonazzola, E. Gourgoulhon, and J-A. Marck, in *Relativistic Gravitation and Gravitational Radiation*, edited by J-A. Marck and J.-P. Lasota (Cambridge University Press, Cambridge, England, 1997).
- [3] S. Bonazzola and J-A. Marck, *Astron. Astrophys.* **267**, 623 (1993).
- [4] E. Gourgoulhon, *Astron. Astrophys.* **252**, 651 (1991).
- [5] E. Gourgoulhon and P. Haensel, *Astron. Astrophys.* **271**, 187 (1993).
- [6] E. Gourgoulhon, P. Haensel, and D. Gondek, *Astron. Astrophys.* **294**, 747 (1995).
- [7] J. Novak, *Phys. Rev. D* **57**, 4789 (1998).
- [8] J-A. Marck, S. Bonazzola, and A. Lioure, *Astron. Astrophys.* **306**, 666 (1996).
- [9] S. Bonazzola, E. Gourgoulhon, M. Salgado, and J-A. Marck, *Astron. Astrophys.* **278**, 421 (1993).
- [10] M. Salgado, S. Bonazzola, E. Gourgoulhon, and P. Haensel, *Astron. Astrophys.* **291**, 155 (1994).
- [11] M. Salgado, S. Bonazzola, E. Gourgoulhon, and P. Haensel, *Astron. Astrophys., Suppl. Ser.* **108**, 455 (1994).
- [12] P. Haensel, S. Bonazzola, and M. Salgado, *Astron. Astrophys.* **296**, 745 (1995).
- [13] M. Bocquet, S. Bonazzola, E. Gourgoulhon, and J. Novak, *Astron. Astrophys.* **301**, 757 (1995).
- [14] P. Haensel and S. Bonazzola, *Astron. Astrophys.* **314**, 1017 (1996).
- [15] S. Bonazzola and E. Gourgoulhon, *Astron. Astrophys.* **312**, 675 (1996).
- [16] S. Bonazzola, J. Friebe, and E. Gourgoulhon, *Astrophys. J.* **460**, 379 (1996).
- [17] S. Bonazzola, J. Friebe, and E. Gourgoulhon, *Astron. Astrophys.* **331**, 280 (1998).
- [18] J-O. Goussard, Ph.D. thesis, Université de Paris 7, 1997.
- [19] J-O. Goussard, P. Haensel, and J.L. Zdunik, *Astron. Astrophys.* **321**, 822 (1997).
- [20] J-O. Goussard, P. Haensel, and J.L. Zdunik, *Astron. Astrophys.* **330**, 1005 (1998).
- [21] D. Gottlieb and S.A. Orszag, *Numerical Analysis of Spectral Methods: Theory and Applications* (Society for Industrial and Applied Mathematics, Philadelphia, 1977).
- [22] C. Canuto, M.Y. Hussaini, A. Quarteroni, and T.A. Zang, *Spectral Methods in Fluid Dynamics* (Springer-Verlag, Berlin, 1988).
- [23] Y. Eriguchi and E. Müller, *Astron. Astrophys.* **146**, 260 (1985).
- [24] Y. Eriguchi and E. Müller, *Astron. Astrophys.* **248**, 435 (1991).
- [25] K. Uryu and Y. Eriguchi, *Mon. Not. R. Astron. Soc.* **282**, 653 (1996).
- [26] S. Bonazzola, E. Gourgoulhon, and J-A. Marck, *J. Comput. Appl. Math.* (to be published).
- [27] S. Bonazzola and J-A. Marck, *J. Comput. Phys.* **87**, 201 (1990).
- [28] S. Bonazzola and E. Gourgoulhon, in *Relativistic Gravitation and Gravitational Radiation* [2].
- [29] U.M. Schaudt and H. Pfister, *Phys. Rev. Lett.* **77**, 3284 (1996).
- [30] S. Chandrasekhar, *Ellipsoidal Figures of Equilibrium* (Yale University Press, New Haven, 1969).
- [31] S. Bonazzola and E. Gourgoulhon, *Class. Quantum Grav.* **11**, 1775 (1994).
- [32] S. Bonazzola and E. Gourgoulhon, in *Relativity in General*, edited by J. Diaz Alonso and M. Lorente Paramo (Editions Frontières, Gif-sur-Yvette, France, 1994).
- [33] S. Wolfram, *Mathematica, a System for Doing Mathematics by Computer* (Addison-Wesley, Reading, Massachusetts, 1992).